

The N-terminus of hTERT contains a DNA-binding domain and is required for telomerase activity and cellular immortalization

David C. F. Sealey^{1,2,3}, Le Zheng^{1,3}, Michael A. S. Taboski^{1,2,3}, Jennifer Cruickshank^{2,3}, Mitsuhiro Ikura^{1,3} and Lea A. Harrington^{1,2,3,4,*}

¹Department of Medical Biophysics, University of Toronto, ²Campbell Family Institute for Breast Cancer Research, ³Ontario Cancer Institute, University Health Network, Toronto, Ontario, M5G 2C1, Canada and ⁴Wellcome Trust Centre for Cell Biology, University of Edinburgh, Edinburgh, EH9 3JR, UK

Received August 6, 2009; Revised November 20, 2009; Accepted November 24, 2009

ABSTRACT

Telomerase defers the onset of telomere damage-induced signaling and cellular senescence by adding DNA onto chromosome ends. The ability of telomerase to elongate single-stranded telomeric DNA depends on the reverse transcriptase domain of TERT, and also relies on protein:DNA contacts outside the active site. We purified the N-terminus of human TERT (hTEN) from *Escherichia coli*, and found that it binds DNA with a preference for telomeric sequence of a certain length and register. hTEN interacted with the C-terminus of hTERT *in trans* to reconstitute enzymatic activity *in vitro*. Mutational analysis of hTEN revealed that amino acids Y18 and Q169 were required for telomerase activity *in vitro*, but not for the interaction with telomere DNA or the C-terminus. These mutants did not reconstitute telomerase activity in cells, maintain telomere length, or extend cellular lifespan. In addition, we found that T116/T117/S118, while dispensable *in vitro*, were required for cellular immortalization. Thus, the interactions of hTEN with telomere DNA and the C-terminus of hTERT are functionally separable from the role of hTEN in telomere elongation activity *in vitro* and *in vivo*, suggesting other roles for the protein and nucleic acid interactions of hTEN within, and possibly outside, the telomerase catalytic core.

INTRODUCTION

Telomeres are specialized nucleoprotein structures that form the ends of linear chromosomes in most eukaryotes.

Telomere DNA, which ranges in length from 100 to 300 bp in ciliates and yeasts, 5–15 kbp in humans, and up to 100 kbp in mice, is comprised by a short repeating duplex sequence (5'-TTAGGG-3'/3'-AATCCC-5' in humans) that terminates in a short G-rich single-stranded overhang (1). The G-overhang can invade the duplex at an upstream position to create a large telomeric loop, or T-loop, in a manner that is facilitated by TRF2 (2,3). TRF1 and TRF2 homodimers bind to the telomere duplex and form a platform for other components of the shelterin complex: RAP1, TIN2, TPP1 and POT1. In addition to binding TPP1, POT1 interacts with, and regulates access to the G-overhang (4). TRF2 and POT1 protect the telomere by limiting the activation of ATM and ATR pathways, respectively, and downstream end-processing activities that normally accompany the DNA damage response (5).

Telomeres shorten with every cycle of DNA replication due to the positioning and degradation of the terminal RNA primer involved in generating the daughter lagging strand, and the nucleolytic resection involved in generating the G-overhang (6–9). Human telomeres shorten by ~100 bp/cell division (10). In cells that undergo many cell divisions, telomeres can reach a minimum length that elicits a DNA damage response (11,12). Consequently, cells enter a usually irreversible non-proliferative state termed senescence. The onset of senescence can be indefinitely postponed by the maintenance of telomere length by telomerase (see below).

Telomerase, originally discovered in *Tetrahymena thermophila* by Greider and Blackburn (13), is a reverse transcriptase formed by the telomerase reverse transcriptase (TERT) and the associated telomerase RNA (TR) which bears the template for synthesis of the telomeric G-strand (14–19). The mutation of telomerase components and premature telomere shortening are

*To whom correspondence should be addressed. Tel: +44 131 650 7113; Fax: +44 131 650 5379; Email: l.harrington@ed.ac.uk

associated with syndromes such as dyskeratosis congenita and idiopathic pulmonary fibrosis that may involve the exhaustion of stem cell compartments (20). In many human somatic cell types, hTERT is transcriptionally repressed (15,16,21). In these cells, telomere erosion and the eventual activation of a DNA damage checkpoint act as barriers to tumorigenesis (22). In cells capable of overcoming senescence, further telomere shortening can result in telomere instability, chromosome end-to-end fusion and tumorigenic conversion (23). Notably, cancer cells can divide indefinitely due to the maintenance of telomeres by the activation of hTERT transcription and telomerase activity (16,21,24) [in exceptional cases, telomeres in some cell types can be maintained by the recombination-based alternative lengthening of telomeres (ALT) (25)]. As proof of concept, primary cells transduced with hTERT cDNA gain the ability to maintain telomeres and divide indefinitely (26,27). Thus, telomerase is an attractive target for the development of anti-cancer therapeutics.

The recruitment of telomerase to telomeres is coordinated with DNA replication (28) and is regulated by the shelterin complex. Telomere length is 'counted' by the complement of telomere duplex binding factors and their effectors, such that the probability of elongation of a given telomere is inversely correlated with its length (29–33). In human cells, POT1 negatively regulates telomerase action at the telomere by binding directly to, and possibly concealing the 3' DNA terminus (34–37). POT1 may also positively regulate telomerase action at the telomere; when positioned on DNA upstream of a 3' end *in vitro*, POT1 stimulates telomerase activity (36,38).

TERT contains several evolutionarily conserved domains. Domains in the C-terminal half of hTERT [amino acids (aa) 601–936] share homology with other reverse transcriptases and form the active site of the enzyme (15–17). Domains in the central region of the protein (CP, QFP, T; aa 397–594) bind the TR (39). A conserved N-terminal domain (GQ), identified by multiple sequence alignment of mammalian, yeast, ciliate and plant TERT sequences (40), is separated from the CP domain by a non-conserved region that varies in length between organisms (39). Telomerase exhibits nucleotide addition processivity by adding one nucleotide at a time onto the 3'-end of a DNA primer, up to the 5'-end of the RNA template. While *Saccharomyces cerevisiae* telomerase, for example, has the ability to add only a limited number of telomeric repeats onto a DNA primer *in vitro* (41), human and *T. thermophila* telomerases exhibit an ability to add multiple telomeric repeats without dissociating from the primer (42,43). Observations that the 5'-end of the primer can influence substrate utilization led to the notion that a so-called 'anchor site' outside of the reverse transcriptase domain of TERT contacts the DNA primer upstream of the active site and may facilitate iterative copying and repositioning of the RNA template (44–49). Mounting evidence suggests that the N-terminus of TERT contains this anchor site for DNA (50) that is important for both telomerase activity and repeat addition processivity.

Indeed, subsequent structural determination of the N-terminus of *T. thermophila* TERT revealed a groove

on one side of the domain that may accommodate single-stranded DNA (51). The domain can form crosslinks to single-stranded DNA primers, and removal of the domain or mutation of exposed residues along the groove reduces primer crosslinking and impairs telomere DNA elongation *in vitro* (51–53). The N-termini of *S. cerevisiae* and human TERTs also interact with DNA (40,54,55), and mutations in the region have been identified that impair telomerase activity/processivity and, in some cases, the ability of telomerase to immortalize cells (40,54–63).

In this study, we found that the N-terminus of human TERT (hTEN), expressed and purified from bacteria, exhibited a length- and sequence-dependent affinity for telomeric DNA in an electrophoretic mobility shift assay (EMSA). Human TEN also interacted with, and restored catalytic potential to an hTERT truncation mutant lacking the N-terminus *in trans*. We identified point mutations in hTEN that strongly impaired telomerase activity and the ability of telomerase to immortalize cells in culture, but did not impair the interaction with telomeric DNA or the hTERT C-terminus.

MATERIALS AND METHODS

Expression and purification of recombinant hTERT

To express hTERT in *E. coli*, the DNA sequence encoding hTERT(aa 1–200) was optimized by correcting for *E. coli* codon bias and minimizing mRNA secondary structure (GenScript Corp.). The custom DNA sequence was synthesized (Blue Heron Biotechnology) and subcloned into BamHI and XhoI sites of a modified pET32a vector to create a Thioredoxin(Trx)-HIS6-hTERT(1–200) coding sequence. The fusion protein of ~36 kDa was expressed in BL21(DE3) codon plus *E. coli* (Stratagene). Cells were grown at 37°C to an OD (600) of 1.0 and expression was induced with 0.2 mM IPTG at 15°C overnight. Cells were harvested by centrifugation and frozen at –80°C. Cell pellets were resuspended in lysis buffer (50 mM Tris–Cl pH 7.5, 25% v/v glycerol, 500 mM NaCl, 0.2% v/v NP40, 10 mM imidazole, 1 mM DTT, 0.2 mM TCEP, Roche Complete protease inhibitor cocktail) and incubated with 0.1 mg/ml lysozyme and 0.05 mg/ml DNaseI at 4°C. Cell debris was removed by centrifugation at 26 000g for 30 min. Soluble lysate was incubated with Ni–NTA resin (Qiagen) at 4°C. After washing with 20 column volumes of wash buffer (50 mM Tris–Cl pH 7.5, 25% v/v glycerol, 1.5 M NaCl, 20 mM imidazole, 1 mM DTT, 0.2 mM TCEP), bound proteins were eluted in 50 mM Tris–Cl pH 7.5, 25% v/v glycerol, 500 mM NaCl, 300 mM imidazole (or 50 mM imidazole in Supplementary Figure S1), 1 mM DTT and 0.2 mM TCEP. Trx-HIS6-hTERT(1–200) was further purified by HiTrap SP cation exchange (GE Healthcare) in a buffer of 50 mM Tris–Cl pH 7.5, 25% v/v glycerol, 5 mM DTT, 0.2 mM TCEP with a 0.08–1.0 M NaCl gradient. The protein could not be dialyzed to a low-salt buffer or concentrated without undergoing precipitation. The control Trx-HIS6 protein was expressed from pET32a and purified over Ni–NTA resin.

To analyze protein composition, elution fractions were boiled in SDS-PAGE loading dye and resolved by denaturing electrophoresis alongside the RPN5800 (GE Healthcare) or Benchmark (Invitrogen) molecular weight markers through 4–20% w/v Tris-Glycine Novex gels (Invitrogen). Gels were stained with Deep-Purple Total Protein Stain (GE Healthcare) or Coomassie Brilliant Blue (Fisher Scientific), or transferred to a PVDF membrane (Invitrogen) and subjected to immunoblotting with anti-Trx primary (Novagen) and sheep anti-mouse IgG-HRP secondary (GE Healthcare) antibodies and ECL Plus detection reagents (GE Healthcare). Deep Purple and ECL Plus fluorescent signals were captured below saturation using a Typhoon Trio variable mode imager (GE Healthcare).

Electrophoretic mobility shift assay

Single-stranded DNA bearing the telomeric sequence (TTAGGG)₃ was labeled at the 5'-end with ³²P. Residual γ-³²P-ATP was removed by centrifugation through a G25 spin column (GE Healthcare). DNA was boiled for 5 min and cooled on ice to minimize secondary structures. Each 20 μl binding reaction contained 1 nM ³²P-(TTAGGG)₃, 50 mM Tris-Cl pH 7.5, 15% (Figure 1C) or 17.5% v/v (Figure 4C) glycerol, 450 mM NaCl, 5 mM DTT and recombinant Trx-HIS6-hTERT(1–200) protein. For the heat denaturation control, protein was denatured on a 95–100°C heating block for 5 min then cooled on ice prior to mixture with DNA. Protein-DNA mixtures were incubated for 30 min at room temperature, then resolved at 15 V/cm at 4°C in cold 0.5× TBE through a pre-cooled gel containing 5% w/v 19:1 acrylamide:bisacrylamide, 0.5× TBE and 5% v/v glycerol (Supplementary Figure S1 was conducted under a voltage gradient; see Supplementary Figure S1 legend for details). Gels were dried at 80°C for 1 h and then exposed to a phosphorimager screen which was then scanned on a Typhoon Trio variable mode imager. Intensity of the DNA shift signal was quantified using ImageQuant software (GE Healthcare). For competition assays, unlabeled DNA of different sequence/length was mixed with ³²P-(TTAGGG)₃ prior to the addition of protein. DNA oligonucleotides were obtained from Integrated DNA Technologies after polyacrylamide gel electrophoresis (PAGE) purification.

Reconstitution of telomerase in reticulocyte lysates

Telomerase activity was reconstituted in rabbit reticulocyte lysates (RRL) as described (64,65), with modifications. Human telomerase RNA (hTR) was transcribed *in vitro* using the RiboMax kit (Promega) and gel-purified. Coupled *in vitro* transcription-translation reactions (Promega Corp.) were prepared with 0.01 μg/μl pCR3-FLAG-hTERT-FLAG cDNA and 0.01 μg/μl hTR RNA, and incubated for 90 min at 30°C. To generate hTERT fragments, the following cDNAs were expressed in separate RRL reactions for 60 min: pCR3-FLAG-hTERT(201–1132)-FLAG; pBiEx3-hTERT(1–200)-S-HIS8; pET32a-Trx-HIS6-hTERT(1–200).

To combine fragments, 15–20 μl of each reaction was then mixed and incubated for an additional 60 min. Mock reactions did not contain a cDNA template. RRL mixtures were then diluted to 500 μl with cold CHAPS buffer (0.5% w/v CHAPS, 10 mM Tris-Cl pH 7.5, 10% v/v glycerol, 100 mM NaCl, 1 mM MgCl₂, 1 mM DTT, Roche EDTA-free complete protease inhibitor cocktail) and rocked for 1 h at 4°C. FLAG-tagged complexes were immunoprecipitated with anti-FLAG M2 affinity resin (Sigma) and washed three times with 1 ml cold CHAPS buffer. For PCR-based analysis of telomerase activity, 1 μl of the immunoprecipitate was assayed by the TRAP (described below). The remainder of the pellet was boiled in SDS-PAGE loading dye and proteins were resolved through 4–20% w/v Tris-Glycine Novex gels, transferred to a PVDF membrane (Invitrogen) and subjected to immunoblotting. Primary antibodies employed were as follows: S protein-HRP (Novagen); rabbit anti-Trx antibody (Sigma); and mouse anti-FLAG M2 antibody (Sigma). Secondary antibodies employed were donkey anti-rabbit IgG-HRP and sheep anti-mouse IgG-HRP (GE Healthcare). Reactive bands were detected with ECL Plus reagents (GE Healthcare) and fluorescent signals were captured using a Typhoon Trio variable mode imager. For direct analysis of primer elongation activity, the entire immunoprecipitate was analyzed by the standard elongation (SE) assay (described below).

Telomerase activity assays

Telomerase activity was assessed using the Telomere Repeat Amplification Protocol (TRAP) or SE assay. TRAP assays were performed using the TRAPeze kit (Millipore) with modifications to the manufacturer's protocol. Cell lysate or *in vitro*-reconstituted telomerase was incubated with the TS primer at 30°C for 30 min prior to heat inactivation at 95°C for 2 min. Reactions were held at 95°C while Taq DNA polymerase (New England Biolabs) was added. Primer extension products were amplified through 25 cycles of 30 s at 94°C, 30 s at 50°C and 90 s at 72°C. Twenty microliters of each 50 μl reaction was combined with DNA loading dye and resolved through a 10% w/v 19:1 acrylamide:bisacrylamide gel in 0.6× TBE at 15–20 V/cm. DNA was stained with SYBR Green I (Sigma) and fluorescent signals were captured on a Typhoon Trio variable mode imager.

For SE assays, *in vitro*-reconstituted telomerase was incubated with 200 pmol PAGE-purified (TTAGGG)₃ (IDT), 40 μCi of [α-³²P]-dGTP (Perkin Elmer, 6000 Ci/mmol, 20 mCi/ml) and 1× SEA buffer (2 mM dATP, 2 mM dTTP, 1 mM MgCl₂, 1 mM spermidine, 5 mM β-mercaptoethanol, 50 mM potassium acetate, 50 mM Tris-acetate pH 8.5) in a 40 μl volume for 2 h at 30°C. Samples were treated with RNase A at 37°C for 15 min, followed by Proteinase K at 37°C for 15 min. Samples were phenol:chloroform extracted. ³²P-end-labeled 96-mer DNA (150 cpm) was added to each reaction as a loading control. DNA was precipitated overnight at –20°C by the addition of 1/10 volume sodium acetate

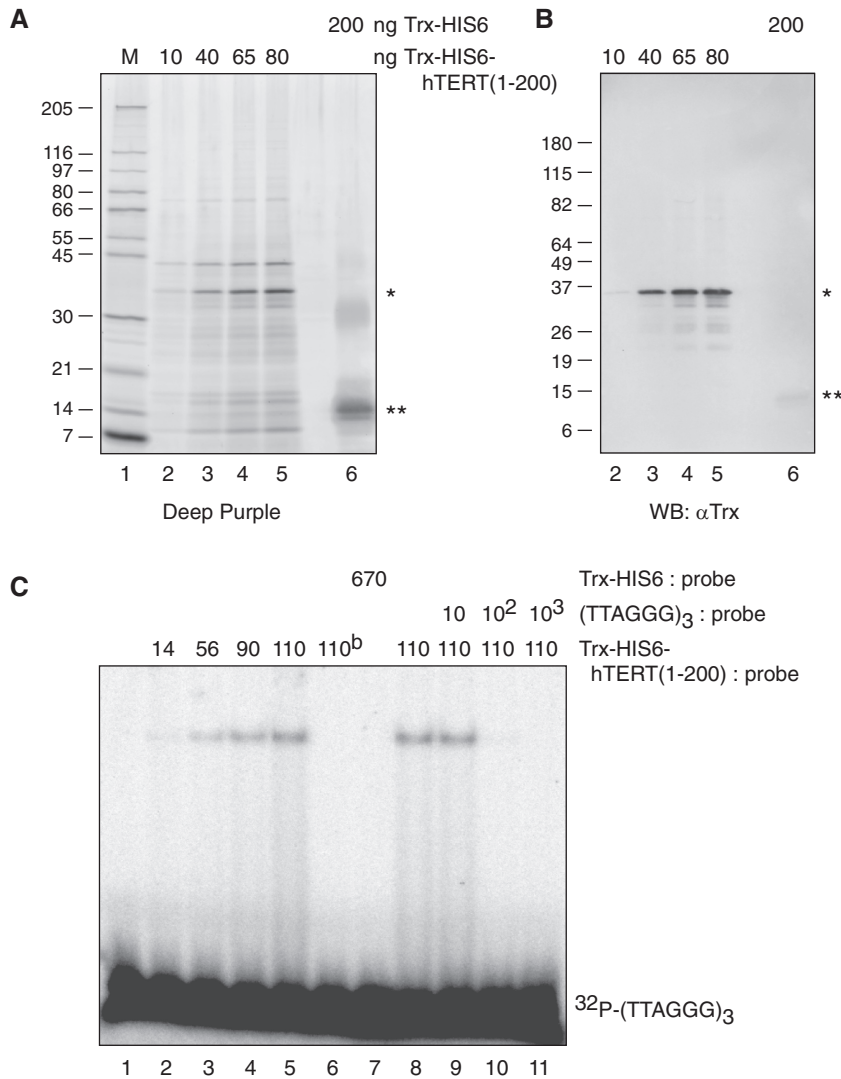


Figure 1. Recombinant hTERT(1–200) interacts with telomeric DNA. **(A)** Analysis of Trx-HIS6-hTERT(1–200) expressed in *E. coli* and purified as described in ‘Materials and Methods’ section. Proteins were boiled in SDS-PAGE loading dye, resolved through a 4–20% w/v Tris–Glycine Novex gel and stained with Deep Purple. The mass (ng) of Trx-HIS6-hTERT(1–200) present in lanes 2–5 was determined by comparing the band intensity of the full length fusion protein (Single asterisk) to the average intensity of bands in the RPN5800 molecular size marker (M, lane 1, 30 ng/band). Molecular mass (kDa) is indicated at the left. Lane 6, Trx-HIS6 (Double asterisk) purified as described in ‘Materials and Methods’ section. **(B)** Proteins prepared as in (A) were transferred to PVDF and immunoblotted with anti-Trx (Novagen) and anti-mouse IgG antibodies. Lane 1 (not shown) contains Benchmark molecular size marker. [Supplementary Figure S3, lanes 7–18 and Figure 3B, lanes 9–10 were probed with a different anti-Trx antibody (Sigma)]. **(C)** EMSA of telomeric DNA. ^{32}P -(TTAGGG) $_3$ was mixed with the following components as described in ‘Materials and Methods’ section: lane 1, DNA alone; lane 2–5, recombinant Trx-HIS6-hTERT(1–200) [same amounts as in (A) and (B), expressed as molar ratio to radiolabeled probe]; lane 6, pre-boiled (^b) Trx-HIS6-hTERT(1–200); lane 7, Trx-HIS6 [same amount as in (A) and (B), expressed as molar ratio to radiolabeled probe]; lanes 9–11, Trx-HIS6-hTERT(1–200) in the presence of unlabeled specific competitor oligonucleotide (at the indicated molar ratio to radiolabeled probe). Lanes 5 and 8 are duplicates. Complexes were resolved by native polyacrylamide gel electrophoresis.

pH 5.2, two volumes cold ethanol and 5 μg GenElute linear polyacrylamide. DNA was pelleted by centrifugation and resuspended in 3 μl gel loading buffer (100% v/v formamide, 0.6 \times TBE). Samples were boiled for 3 min and resolved by electrophoresis in 0.6 \times TBE through a 10% w/v denaturing polyacrylamide gel (29:1, acrylamide:bisacrylamide, 7M urea, 0.6 \times TBE). The gel was dried at 80°C for 1 h, and then exposed to a phosphorimager screen which was then scanned on a Typhoon Trio variable mode imager.

Mutagenesis of hTERT(1–200)

The structure-based sequence alignment of the N-terminus of TERT (51) was used as a guide to select residues in hTERT(1–200) that may be exposed to the surface of the protein (refer to Supplementary Figure S4). The design of PCR primers for site-directed mutagenesis was aided by The Primer Generator (66). Primers were obtained from Operon and IDT. The incorporation of intended mutations into the cDNA (and the absence of unwanted mutations) was confirmed by DNA sequencing.

Generation and passaging of stable cell lines

pcDNA3.1(hyg)-hTERT vectors were linearized with SspI, treated with calf intestinal phosphatase (New England Biolabs), and then gel-purified. Human embryonic kidney HA5 cells were transduced with either wild-type or mutant hTERT DNA using FuGENE6 transfection reagent (Roche). Cells were grown in alpha-Minimal Essential Medium (α -MEM) containing 10% v/v fetal bovine serum and 2 mM L-glutamine, and then selected with 200 μ g/ml (Supplementary Figure S5) or 100 μ g/ml hygromycin (Figure 5). Cells undergoing mock transfection (with no DNA) did not survive selection. After 4–5 weeks of selection, colonies were treated with TrypLE Express (Invitrogen) and pooled. Polyclonal populations were passaged in media containing hygromycin by plating 2×10^5 cells in a 10 cm plate at regular intervals. The number of cumulative population doublings at each passage was determined by the formula as described (67). The experiment was performed with late-passage cells approaching crisis (Supplementary Figure S5), and also with cells at an earlier passage (Figure 5). Apoptosis was assessed using the TiterTACS assay (R&D Systems) and by visual inspection of cellular morphology by microscopy.

Protein extraction

Cells were washed with ice-cold PBS and dislodged from tissue culture plates using a cell scraper. Cells were resuspended and lysed in 4–5 volumes of ice-cold CHAPS buffer (0.5% w/v CHAPS, 10 mM Tris-Cl pH 7.5, 10% v/v glycerol, 1 mM MgCl₂, 5 mM β -mercaptoethanol, Roche EDTA-free Complete protease inhibitor and 400 U Roche RNase Inhibitor) for 30 min on ice. Insoluble material was pelleted by centrifugation at 13 000 r.p.m. for 30 min. The protein concentration of the cleared whole cell extract was determined by the Bradford Assay (Bio-Rad).

Analysis of mRNA by RT-PCR

Total RNA was isolated from cells using TRIzol reagent (Invitrogen), and then treated with DNase I (Roche). cDNA was generated from RNA using Superscript II reverse transcriptase (Invitrogen) and random hexamer primers (Invitrogen). Residual RNA was removed from cDNA products using RNase H (Invitrogen). cDNAs were amplified by PCR using Taq DNA polymerase (New England Biolabs) under the following conditions: 94°C for 5 min, followed by 32 cycles of 94°C for 45 s, 57°C for 45 s and 72°C for 1 min, followed by a final extension of 72°C for 4 min. The following gene-specific primers were used: *GAPDH*, 5'-CGGAGTCAACGGATTTGGT CGTAT-3' and 5'-TGCTAAGCAGTTGGTGGTGCGAG GA-3'; *hTERT*, 5'-AAGTTCCTGCACTGGCTGATGA G-3' and 5'-TCGTAGTTGAGCACGCTGAACAG-3'; hygromycin resistance (*HYG-R*), 5'-CGCAAGGAATCG GTCAATAC-3' and 5'-ACATTGTTGGAGCCGAAA TC-3'. DNA was resolved through a 0.8% w/v agarose gel, stained with ethidium bromide, and imaged on a Typhoon Trio variable mode imager.

Telomere length analysis

Genomic DNA was isolated from cells using the DNeasy kit (Qiagen) and digested with RsaI and HinfI. Restriction fragments were resolved through a 0.5% w/v agarose gel at 45 V (2 V/cm) for 24 h. DNA was denatured in buffer containing 0.5 M NaOH, 1.5 mM NaCl for 30 min, and neutralized in buffer containing 1.5 M NaCl, 0.5 mM Tris-Cl pH 7.5 for 30 min. DNA was transferred to Hybond N+ membrane in 20 \times SSC. Following transfer, DNA was UV-crosslinked to the membrane, which was then rinsed in 2 \times SSC. Telomeric DNA was hybridized to a ³²P 5'-end-labeled (CCCTAA)₃ probe in Church buffer (0.5 M NaPO₄ pH 7.2, 1% w/v BSA, 7% w/v SDS, 1 mM EDTA), then washed with 1 \times SSC, 0.1% w/v SDS. The membrane was exposed to a phosphorimager screen which was then scanned using a Typhoon Trio variable mode imager. The weighted mean of telomere length in each lane was calculated according the following formula, as previously described (68): $\Sigma(\text{OD}_i)/\Sigma(\text{OD}_i/L_i)$, where OD_{*i*} is the signal intensity and L_{*i*} is the length in nucleotides of DNA at position *i* as determined by comparison to the molecular mass standards.

RESULTS

Production of recombinant hTERT(1–200) in a bacterial expression system

The N-terminus of *T. thermophila* TERT contains a DNA-binding domain (51–53). Mutations in this region impair telomerase activity, as do mutations in the equivalent region of hTERT (55,58–63). Thus, this region has been dubbed the telomerase essential N-terminal (TEN) domain (51). Although the N-terminus of TERT contains a region of homology (GQ), the sequence conservation between human and *T. thermophila* TERTs in this region is especially low. Unpurified hTERT(aa 1–300) and hTERT(1–350) generated in reticulocyte lysates can be captured onto biotinylated telomeric DNA in a neutravidin pull-down assay [(55), D.C.F. Sealey and L.A. Harrington, unpublished results]. To clarify this apparent hTERT–DNA interaction, we developed a strategy to produce recombinant hTERT in bacteria.

We expressed Trx-HIS6-hTERT(1–200) in *E. coli* and, despite a low expression level and limited solubility (<5% of expressed protein was recovered in the soluble fraction of the cell lysate), we purified the protein over two chromatographic steps to a modest degree of homogeneity (see 'Materials and Methods' section). The fusion protein was detected at the expected size of 36 kDa (Figure 1A). The presence of Trx fused at the N-terminus was confirmed by western blotting (Figure 1B) and the identity of TERT was confirmed by tandem mass spectrometry (MS) (T. Goh and T. LeBihan, data not shown). Minor bands at higher molecular weights were identified as the bacterial chaperones DNaK and DNaJ and the translation elongation factor Tu (T. Goh and D.C.F. Sealey data not shown). The majority of peptides derived from the lower molecular weight bands, some of which were reactive to

anti-Trx antibody, corresponded to fragments of Trx-HIS6-hTERT(1–200) based on MS analysis (Figure 1B and data not shown). The purity of full length Trx-HIS6-hTERT(1–200) in a typical purification was determined to be 75% based on Coomassie staining (data not shown). Based on Deep Purple staining (which is more sensitive than Coomassie), purity was determined to range from 20% (Figure 1A) to 40% (Figure 4A).

hTERT(1–200) interacts with telomeric DNA *in vitro*

To determine whether hTERT(1–200) interacts with DNA, we performed EMSAs. Recombinant Trx-HIS6-hTERT(1–200) was mixed with radiolabeled single-stranded DNA oligonucleotides containing three full telomeric repeats and subjected to native polyacrylamide gel electrophoresis. A slower mobility complex contained labeled DNA, and this complex increased in intensity upon addition of increasing amounts of protein (Figure 1C). The DNA shift reached a maximum when the binding mixture contained 450 mM NaCl, and persisted in 1 M NaCl (data not shown). Heat denaturation of the protein preparation inactivated the apparent DNA-binding activity (Figure 1C, lane 6). The gel shift observed with radiolabeled DNA was, as expected, competed by an excess molar ratio of unlabeled, specific oligonucleotide (Figure 1C, lanes 9–11). An extract prepared from cells expressing Trx-HIS6 and purified over Ni-NTA resin (in the same manner as Trx-HIS6-hTERT) did not interact with telomeric DNA (Figure 1C, lane 7). Furthermore, the electrophoretic mobility of telomeric DNA in complex with Trx-HIS6-hTERT [or another hTERT(1–200)-S-HIS fusion protein] was altered upon the addition of anti-HIS antibody but not other antibodies. Specifically, a slower mobility complex disappeared upon incubation with increasing concentrations of anti-HIS antibody, concomitant with the enrichment or appearance of faster mobility complexes (Supplementary Figure S1). Antibodies specific to their cognate protein often elicit a ‘supershift’ (i.e. retardation of mobility) upon binding to the DNA:protein complex. Although not as common, antibody recognition can perturb the intact nucleoprotein complex leading to the disappearance of complexes, or appearance of faster mobility complexes, owing to an alteration of relative DNA:protein stoichiometry (69–71). These data show that hTEN was present in the telomeric DNA complex, and argue for a specific interaction between the N-terminus of hTERT and telomeric DNA.

hTERT(1–200) interacts preferentially with telomeric DNA of a particular register and sufficient length

To determine the DNA-binding specificity of the hTEN complex, we tested the ability of unlabeled competitor DNA oligonucleotides of different length and/or telomeric register to compete with labeled (TTAGGG)₃ for binding to Trx-HIS6-hTERT(1–200), and expressed the relative apparent binding affinities as the amount of

oligonucleotide required to reduce the signal intensity of the mobility shift by 50% (Figure 2, Supplementary Figure S2 and data not shown). Single-stranded oligonucleotides 18 nucleotides (nt) in length did not require a specific 5'- or 3'-end in the telomeric register to facilitate binding (Figure 2A, compare oligonucleotides I, II). Oligonucleotides ending in GGG required at least 13 nt of telomeric sequence to bind comparably to the 18 nt (TTAGGG)₃ probe (I, III, IV, V). For oligonucleotides 13 nt in length, a specific telomeric register was preferred: in decreasing order of apparent affinity, oligonucleotides that terminated in GGG, GG and G (IV, VI, IX). Reducing the length to 12 nt in any register reduced the apparent binding affinity (compare IV and V; VI and VII; IX and X). Oligonucleotides 12 nt in length were recognized when containing, in decreasing order of apparent affinity, terminal GG, GGG, G and no G (VII, V, X, XIII). Reducing oligonucleotide length to 11 nt reduced the apparent affinity for DNA ending in GG (VII and VIII); when ending in G, a further decrease in apparent affinity was observed only upon decreasing the length to 10 nt (X, XI, XII). Surprisingly, for oligonucleotides ending in TTA, 11 nt (but not 10 nt) bound with a greater apparent affinity than did 12 nt (XIII, XIV, XV). From this dataset, we conclude that single-stranded telomeric DNA 13 nt in length and terminating in GGG or GG was a preferred substrate for hTEN binding (IV, VI), whereas oligonucleotides of this length with different telomeric registers, or shorter oligonucleotides, did not bind with a comparable apparent affinity.

To determine the sequence specificity of the DNA interaction, we performed another set of competition experiments with oligonucleotides containing non-telomeric substitutions (Figure 2B). Telomeric DNA 18 nt in length in which the middle G at position 11 was replaced with C had a 7-fold lower apparent affinity for hTEN (compare I and I.C11). For telomeric DNA 13 nt in length and ending in a GG register (VI), replacing G with C significantly reduced apparent affinity at some positions (VI.C1, C6, C7, C12, C13) but not others (VI.C2, C8). Interestingly, replacing the central GGG with TTA did not reduce apparent affinity (VI.TA6), whereas replacing the GG with TA at the 5'- and 3'-ends did reduce apparent affinity (VI.TA1.12). Combining these central, 5' and 3' GG-to-TA replacements reduced apparent affinity (VI.TA1.6.12), suggesting that GG residues form critical contacts with hTEN and that the central GGG, while not required, does stabilize the interaction in the absence of other G contacts. Inverting the GGG and TA positions across the 13 nt also reduced relative binding affinity (VI.INVERT), again suggesting that GG ‘bookends’ facilitate the hTEN:DNA interaction, and that the relative positions of internal G residues are also important. Taken together, these data indicate that the interaction of hTEN with oligonucleotides 13 nt in length depends on G-rich character at certain positions—a demonstration of telomere sequence specificity (Figure 2B, lower), and in keeping with previous observations on the preferred substrate composition for elongation by telomerase (see ‘Discussion’ section).

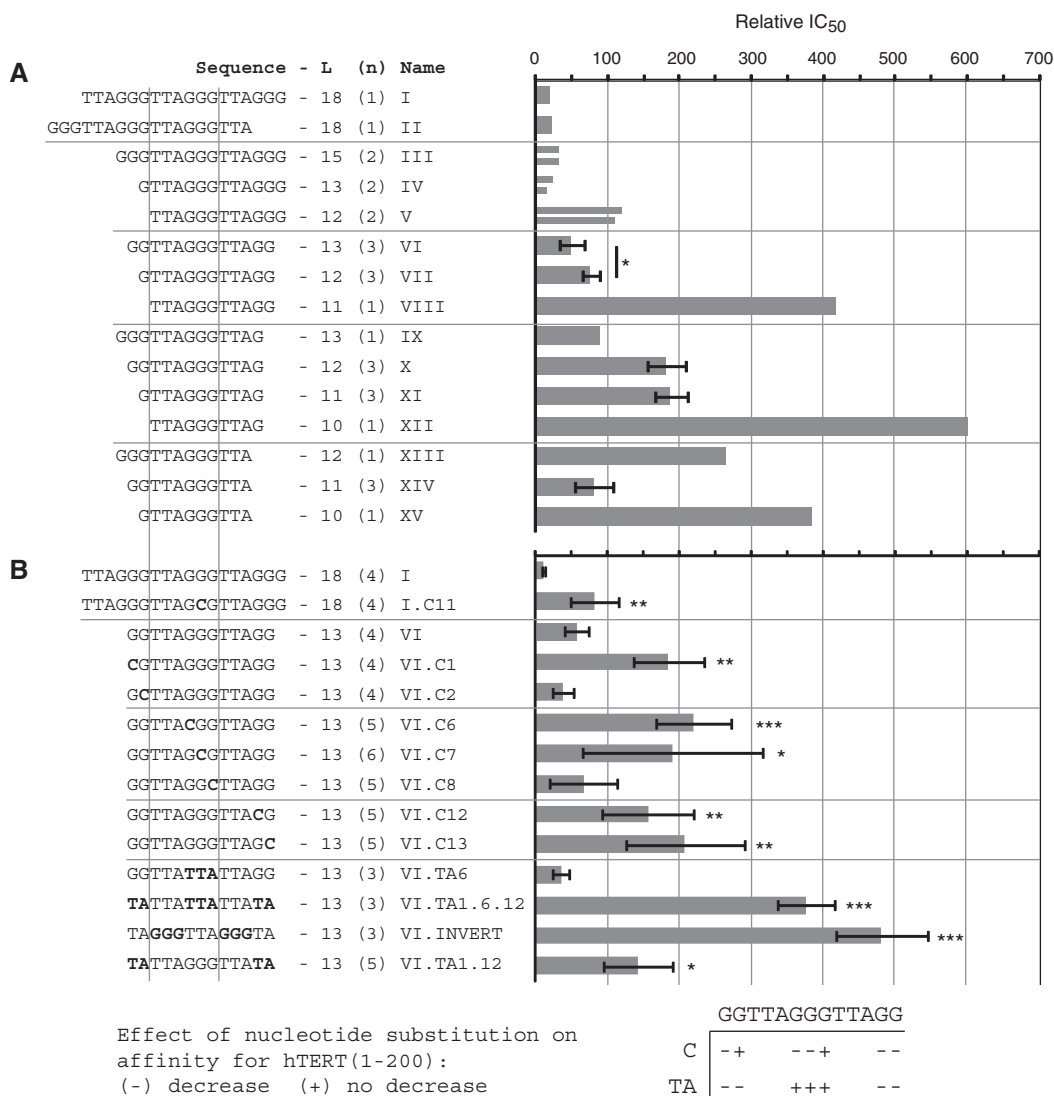


Figure 2. DNA sequence and length preferences for binding of hTERT(1–200). (A and B) ³²P-(TTAGGG)₃ was incubated with a molar excess of unlabeled competitor prior to addition of Trx-HIS6-hTERT(1–200). Complexes were resolved by EMSA. (An example of the raw data is shown in Supplementary Figure S2.) X-axis indicates the molar ratio of unlabeled competitor oligonucleotide relative to ³²P-(TTAGGG)₃ required to reduce the Trx-HIS6-hTERT(1–200)-dependent gel shift signal by 50% (relative IC₅₀). Y-axis indicates the sequence, length (L), number of replicates (n) and name of oligonucleotides tested. To confirm the reproducibility of results, (A) and (B) were performed with different elution fractions from the same purification. (A) Relative apparent binding affinities of DNA oligonucleotides with different length and telomeric register. A one-tailed *t*-test for samples with equal variance was used to conclude significance (**P* < 0.05; compare VI and VII). (B) Relative apparent binding affinities of telomeric DNA oligonucleotides with non-telomeric substitutions. A two-tailed *t*-test for samples with unequal variance was used to identify significant decreases in affinity relative to the unmodified telomeric oligonucleotide of identical length (**P* < 0.05, ***P* < 0.025, ****P* < 0.006). The bottom schematic indicates positions at which nucleotide substitutions decrease (–) or do not decrease (+) the interaction with hTERT(1–200).

hTERT(1–200) can restore activity to the inactive hTERT(201–1132) fragment *in trans*

N-terminal fragments of hTERT can restore enzymatic function, *in trans*, to inactive fragments of the remainder of hTERT in combination with hTR (59,62). Since hTERT(201–1132) possesses an activity defect (58), we reasoned that providing the hTEN DNA-binding domain *in trans* may restore its activity. We reconstituted telomerase activity in RRLs by expressing FLAG-hTERT cDNA in the presence of hTR, and assayed anti-FLAG immunoprecipitates for telomerase activity (see ‘Materials and Methods’ section). Whereas wild-type hTERT displayed a characteristic ability to generate long extension

products (Supplementary Figure S3, lane 1; and Figure 3A and B, lane 1), removal of the first 200 amino acids nearly abolished this activity (Supplementary Figure S3, lane 2; and Figure 3A and B, lane 2), as demonstrated previously (58,59). However, when mixed with hTERT(1–200) (containing Trx or an S-tag at the N- or C-terminus, respectively) after separate translation in RRL, the two fragments interacted with one another and catalytic activity was restored (Supplementary Figure S3, lanes 3 and 7; Figure 3A, lane 3; Figure 3B, lanes 3 and 9). (Note: hTR was not required for the interaction of hTERT N- and C-termini; Supplementary Figure S3, lanes 5, 13 and 14.) Therefore, hTERT(1–200) is essential for

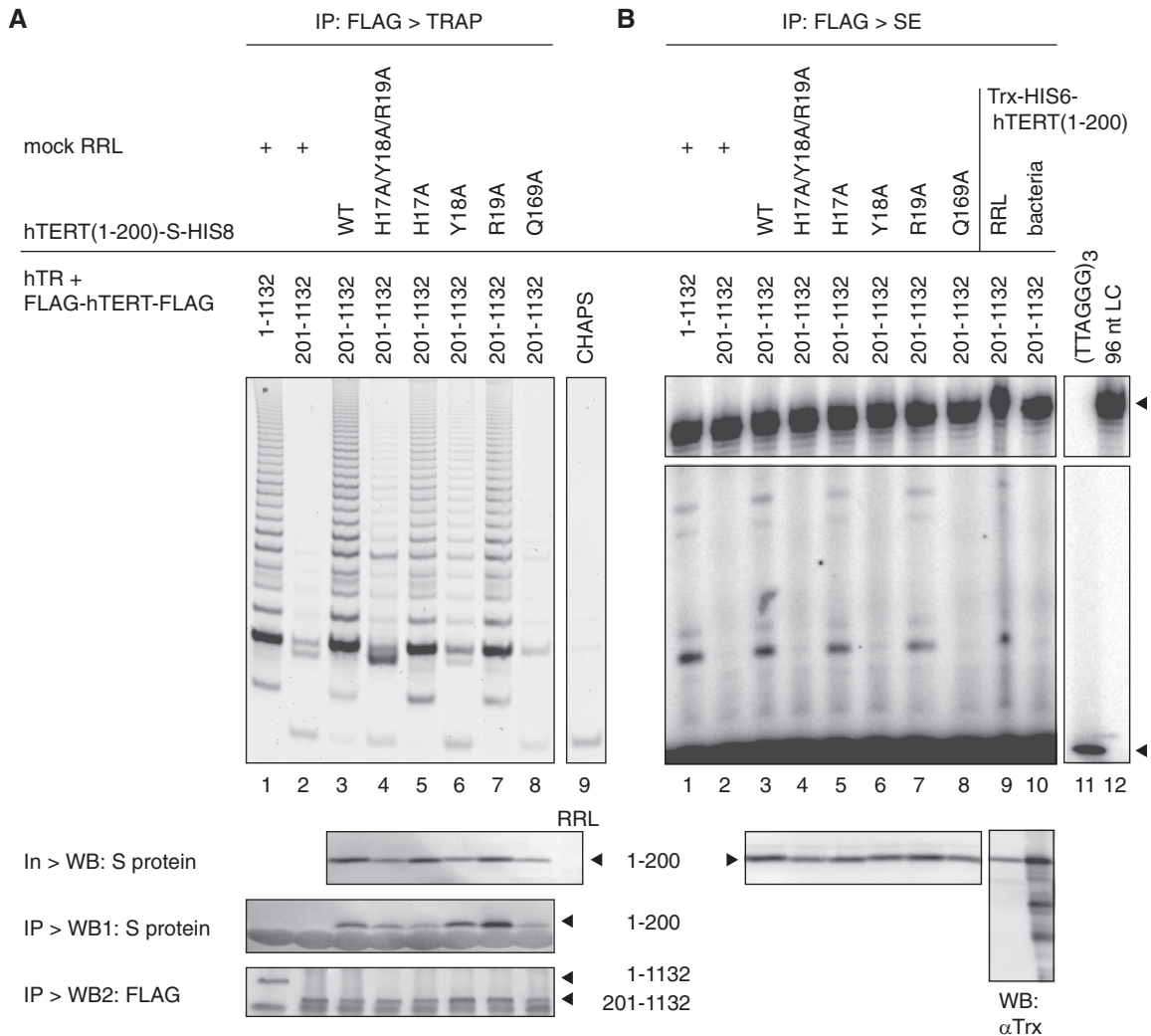


Figure 3. hTERT(1-200) rescues the activity defect of hTERT(201-1132) in a Y18- and Q169-dependent manner. FLAG-tagged hTERT(201-1132) was mixed with mock RRL (lane 2), wild-type (lane 3) or mutant hTERT(1-200)-S-HIS8 containing substitutions at the indicated positions (lanes 4-8) and immunoprecipitated onto anti-FLAG resin (IP). FLAG-hTERT(1-1132) was mixed with mock RRL as a positive control (lane 1). (A) Telomerase activity in the IPs was assessed by TRAP. Irrelevant lanes between 8 and 9 were removed. Buffer alone (CHAPS) was assayed as a negative control (lane 9). Immunoprecipitates (IP) were analyzed by western blotting using S protein-HRP (WB1), followed by anti-FLAG M2 and anti-mouse IgG antibodies (WB2). Fifteen percent of input protein (In) was analyzed on a separate blot with S protein-HRP. (B) Telomerase activity in the IPs was analyzed using a radioactive, linear standard elongation (SE) telomerase assay. Lane 9, 10, Trx-HIS6-hTERT(1-200) produced in RRL or bacteria, respectively. Lane 11, position of the (TTAGGG)₃ DNA oligonucleotide upon 5'-end-labeling with ³²P (bottom arrowhead). Lane 12, 96 nt loading control (top arrowhead) that was added to each reaction prior to the recovery of extension products. Bottom panel: 15% of input protein was analyzed by western blotting using S protein-HRP (lanes 3-8). Fifteen and 60% of input protein were analyzed in lanes 9 and 10, respectively, using anti-Trx (Sigma) and anti-rabbit IgG-HRP antibodies.

telomerase activity *in vitro*, and can function as a separable domain to restore activity to an inactive fragment of hTERT. While recombinant, purified Trx-HIS-hTERT(1-200) interacted with hTERT(201-1132), this purified preparation was unable to regenerate in activity in combination with hTERT(201-1132) (Supplementary Figure S3, lanes 8, 14 and 17; Figure 3B, lane 10) (see 'Discussion' section).

Identification of amino acids in hTERT(1-200) that are critical for telomerase activity *in vitro*

Although the first 200 amino acids of human and *T. thermophila* TERTs share <15% identity and 25% similarity, the N-terminus of hTERT may still adopt a similar three-dimensional fold. Guided by the sequence alignment

of the N-terminus of hTERT to the *T. thermophila* TERT TEN domain structure (51), we generated point mutations in acidic, basic and polar residues in hTEN that are potentially exposed to the surface, and assayed mutants in the context of hTEN for the ability to restore function to hTERT(201-1132) (refer to Supplementary Figure S4). Many of the mutations, including T116A/T117A/S118A, exhibited no discernible effect on telomerase activity or the ability to interact with hTERT(201-1132) + hTR (Figure 3A and B, lanes 5 and 7, and data not shown; summarized in Table 1). In contrast, mutation of Q169A in hTERT(1-200)-S-HIS8 or Trx-HIS6-hTERT(1-200) impaired telomerase function as assayed by TRAP (Figure 3A, lane 8 and data not shown; Table 1).

Table 1. Summary of hTERT mutant phenotypes

Allele	Telomerase activity ^a		DNA binding ^b	Cell lifespan extension ^c	Predicted surface ^d
	TRAP	SE			
Normal activity, binds DNA, extends cellular lifespan					
WT	+ (17, 4 ^e)	+ (7, 1 ^e)	+	+ (2)	
Normal activity, binds DNA, does not extend cellular lifespan					
T116A/T117A/S118A	+ (3)	+ (1)	+	– (2)	A/B
Defective activity, binds DNA, does not extend cellular lifespan					
H17A/Y18A/R19A	– (8)	– (4)		– (3)	A/B.G
Y18A	– (3)	– (4)	+	? (1)	A/B.G
Q169A	– (10, 2 ^e)	– (3)	+	– (3)	A.G
Normal activity (not tested: DNA binding, cellular lifespan extension)					
R15A/S16A	+ (3)	+ (1)			A/B.G
H17A	+ (5)	+ (4)	A/B
R19A	+ (5)	+ (4)			A/B.G
R29A/R30A	+ (3)	+ (2)			B
Q34A/R37A	+ (5)	+ (1)	B
R48A	+ (3)	+ (1)			A/B
Q53A	+ (3)	+ (1)			A/B
S70A/R72A/Q73A	+ (3)	+ (1)	B
D105A	+ (3)	+ (1)			B
E113A	+ (3)	+ (1)			A
S121A/Y122A	+ (3)	+ (1)	A
D129A	+ (3)	+ (1)			A.G
S134A	+ (3)	+ (1)			A
R155A	+ (3)	+ (1)	B
T182A/Q183A/R185A	+ (5)	+ (1)			A/B.G
H189A/S191A	+ (3)	+ (2)			A/B.G

^a '+' no defect or '–' defect. Phenotype representative of (n) experimental replicates.

^b Telomerase was reconstituted by mixing RRL-expressed hTERT(1–200)-S-HIS8 with FLAG-hTERT(201–1132)-FLAG in the presence of hTR.

^c Trx-HIS6-hTERT(1–200), purified from bacteria, was mixed with (TTAGGG)₃ and complexes were analyzed by electrophoretic mobility shift assay (EMSA).

^d HA5 cells stably expressing hTERT(1–1132) were passaged under selection. (?) indicates that expression of the Y18A mutant was lost during the experiment, precluding a conclusion regarding loss of function.

^e See Supplementary Figure S4. Predicted surface position based on alignment of the hTERT sequence to the structure of the *T. thermophila* TERT TEN domain (51). Side 'A' includes the putative DNA-binding groove. Side 'B' faces opposite Side 'A.' A/B represents an edge between both sides. G indicates a location in/near the putative DNA-binding groove. Refer to 'Materials and Methods' section for additional details.

^f Telomerase was reconstituted by mixing RRL-expressed Trx-HIS6-hTERT(1–200) with FLAG-hTERT(201–1132)-FLAG in the presence of hTR. Anti-FLAG immunoprecipitates were assayed for telomerase activity by TRAP or SE protocols.

Also, Q169A rendered telomerase unable to catalyze nucleotide addition in the SE assay—an unequivocal indication that Q169 is required for catalytic activity (Figure 3B, lane 8 and data not shown; Table 1) similar to the requirement for Q168 in *T. thermophila* TERT (51). The H17A/Y18A/R19A mutant displayed a similar inability to elongate telomeric DNA, although the defect by TRAP was not as pronounced (Figure 3A and B, lane 4; Table 1). The defect of the triple mutant was attributed to a single amino acid change at Y18, but not H17 or R19 (Figure 3A and B, lanes 5–7). None of the mutations described above disrupted the interaction with hTERT(201–1132) + hTR (Figure 3A).

Y18 or Q169 are dispensable for the interaction of hTERT(1–200) with DNA

To further study the effect of hTEN mutation on the biochemical activities of telomerase, we produced hTEN mutants in bacteria alongside wild-type hTEN in the same manner as described above. Purifications of Trx-HIS6-hTERT(1–200) wild-type, Y18A, T116A/

T117A/S118A and Q169A contained a prominent band at the expected size that was recognized by anti-Trx antibody (Figure 4A and B). Lower molecular weight fragments of the fusion protein co-purified with the intact protein, as in our purification of wild-type hTEN (see also Figure 1B). Only Q169A contained a noticeable truncation product at 31 kDa that was recognized by anti-Trx antibody and was present in equal abundance to the full-length 36 kDa fusion protein (Figure 4A and B).

To determine whether residues in hTEN that are required for activity are required for DNA binding, we performed EMSAs with hTEN mutants. As before, Trx-HIS6-hTERT(1–200) shifted the single-stranded telomeric DNA oligonucleotide in a native gel in a concentration-dependent manner (Figure 4C, lanes 2–4). The T116A/T117A/S118A mutant also bound telomeric DNA (Figure 4C, lanes 8–10), which is consistent with the predicted position of these residues on the surface of the domain opposite the putative DNA-binding groove, and an apparent lack of involvement in the catalytic

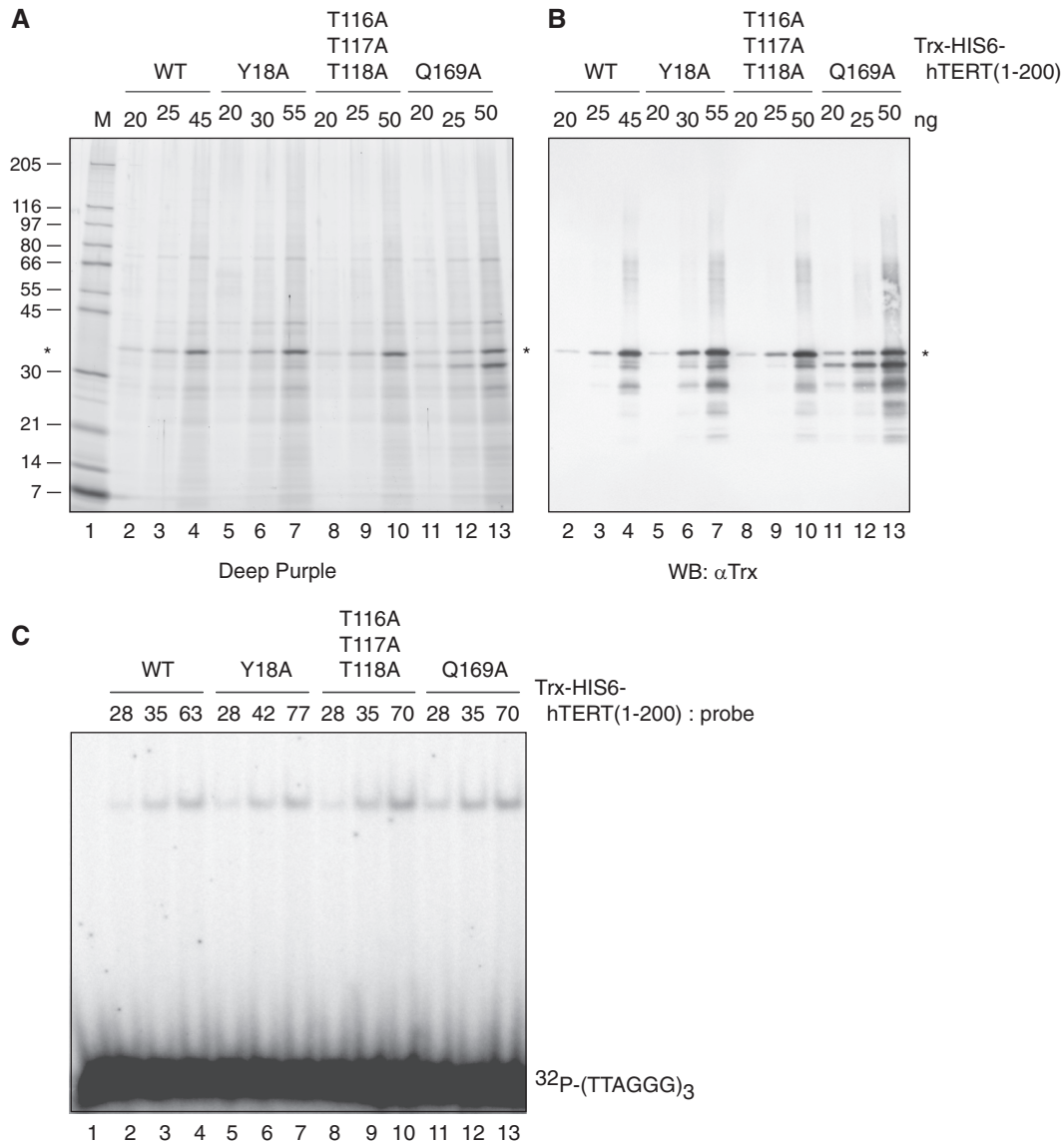


Figure 4. Selected mutations in hTERT(1–200) do not abrogate DNA-binding activity. (A) Analysis of Trx-HIS6-hTERT(1–200) (wild-type or mutant, as indicated) expressed in *E. coli* and purified as described in ‘Materials and Methods’ section. Proteins were boiled in SDS-PAGE loading dye, resolved through a 4–20% w/v Tris–Glycine Novex gel and stained with Deep Purple. The mass (ng) of Trx-HIS6-hTERT(1–200) present in lanes 2–13 was determined by comparing the band intensity of the full-length fusion protein (*) to the average intensity of bands in the RPN5800 molecular size marker (M, lane 1, 30 ng/band). Molecular mass indicated at left (kDa). (B) Proteins prepared as in (A) were transferred to PVDF and immunoblotted with anti-Trx (Novagen) and anti-mouse IgG-HRP antibodies. (C) Electrophoretic mobility shift assay of telomeric DNA. 32 P-(TTAGGG)₃ was mixed with the following components as described in ‘Materials and Methods’ section: lane 1, DNA alone; lanes 2–13, increasing amounts of wild-type or mutant Trx-HIS-hTERT(1–200) [same amounts as in (A) and (B); expressed as molar ratio to radiolabeled probe]. Complexes were resolved by native polyacrylamide gel electrophoresis.

reaction cycle (Table 1, Supplementary Figure S4). Interestingly, mutation of Y18 or Q169, each of which impaired telomerase activity, did not affect the ability of hTEN to bind telomeric DNA (Figure 4C, lanes 5–7, 11–13). One could infer that these residues do not contact DNA, or that these residues may contact DNA (based on their predicted positions in/near the putative DNA-binding groove) but that neither Y18 nor Q169 is the sole determinant of a DNA interaction—at least not to an extent that can be resolved by the EMSA assay. The ability of hTEN(Q169A) to bind telomeric DNA in an EMSA differs from the reduced primer crosslinking

ability of *T. thermophila* TERT(Q168A) (51) (see ‘Discussion’ section).

Residues in hTERT(1–200) are required for telomerase-mediated extension of cellular lifespan

To determine whether Y18 and Q169, as determinants of telomerase activity *in vitro*, are also required for telomerase function in cells, we performed a cellular immortalization experiment. We created polyclonal HA5 cell lines [HA5 is a mortal, SV40-transformed human embryonic kidney cell line that bypasses senescence and

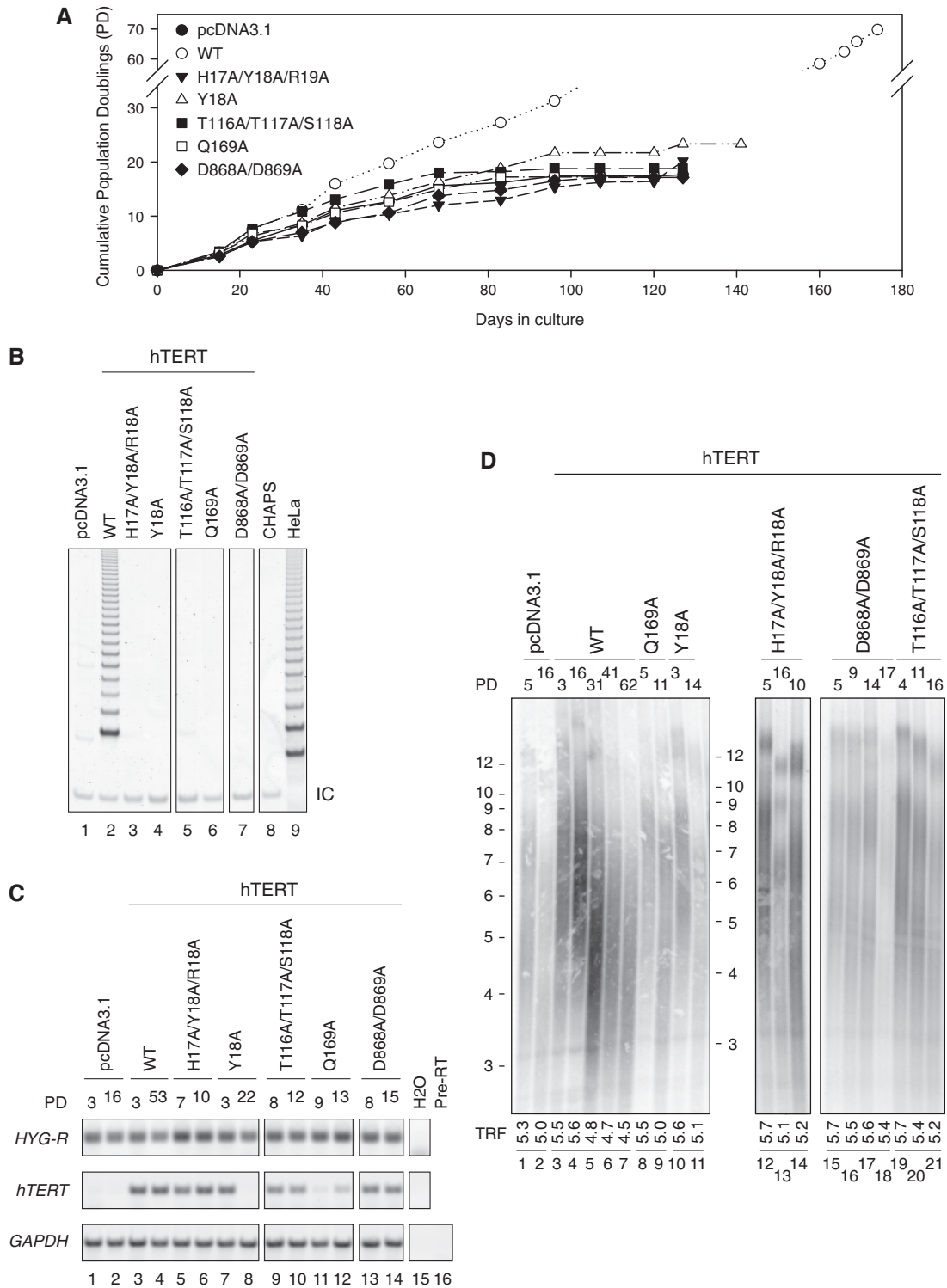


Figure 5. Selected mutations in the N-terminus of hTERT interfere with the ability of telomerase to extend the replicative lifespan of primary human (HA5) cells. **(A)** Polyclonal cell lines containing wild-type or mutant hTERT cDNA (or pcDNA3.1 as a negative control) were derived from HA5 cells (at earlier passage than cells used in Supplementary Figure S5). Cells were passaged under selection with hygromycin. Y-axis contains a break spanning population doublings (PD) 35–55 in order to display the uninterrupted growth of cells expressing wild-type hTERT. **(B)** Lysates of polyclonal cell lines containing wild-type or mutant hTERT cDNA were prepared in CHAPS buffer at Day 35 and assayed for telomerase activity by TRAP. CHAPS buffer was assayed as a negative control (lane 8). HeLa cell lysate was assayed as a positive control (lane 9). IC indicates TRAP internal control product. Lanes containing irrelevant samples were omitted. **(C)** Analysis of *hTERT* mRNA expression level at early and late passage by RT-PCR. Hygromycin resistance (*HYG-R*, upper), *hTERT* (middle) and *GAPDH* cDNAs were amplified using gene-specific primers (refer to ‘Materials and Methods’ section). Lanes containing irrelevant samples were omitted. **(D)** Analysis of the terminal telomere restriction fragments (TRF) at the indicated population doubling (PD) of polyclonal HA5 cell lines receiving wild-type or mutant hTERT. Genomic DNA was isolated, digested with *RsaI* and *HinfI*, and subjected to Southern blotting using a $(CCCTAA)_3$ probe (refer to ‘Materials and Methods’ section). Molecular size (kbp) is shown at left according to the migration of 1 kbp + DNA ladder (not shown). Left, middle and right panels were analyzed separately and aligned according to duplicate samples contained on individual blots (not shown). The weighted mean of telomere length (kbp) is indicated at the bottom of each lane. The presence of an interstitial, cross-hybridizing band at 3 kbp can be used to estimate the relative DNA loading of each lane.

encounters crisis—characterized by telomere instability and apoptosis—and does not undergo spontaneous immortalization (72)] stably expressing wild-type or mutant hTERT, and monitored population doubling levels at regular intervals. Cells that received wild-type hTERT cDNA continued to divide through the duration of the experiment, whereas cells receiving empty vector (pcDNA3.1) or hTERT(D868A/D869A) (mutations that inactivate reverse transcriptase activity) succumbed to apoptosis within ~10 population doublings (Supplementary Figure S5, data not shown), which is consistent with previous observations (17,73). Cells receiving hTERT(H17A/Y18A/R19A) ($n = 2$), Q169A ($n = 2$), or T116A/T117A/S118A mutants ($n = 1$) were also unable to divide beyond 10 population doublings.

To confirm these results, we derived a second set of stable lines from HA5 cells at an earlier passage. As before, cells receiving wild-type hTERT survived through the duration of the experiment. In contrast, cells receiving mutant hTERT cDNA failed to survive beyond 15–20 population doublings (Figure 5A). This delay in reaching crisis relative to HA5 cells transduced at a later passage (Supplementary Figure S5) is in keeping with the different initial telomere lengths of these two populations (10). We assayed telomerase activity in lysates prepared from cells at day 35 in the experiment (Figure 5B). Lysates from cells containing H17A/Y18A/R19A, Y18A, Q169A, or D868A/D869A mutants did not display telomerase activity, which is consistent with the reduced activity of these mutants in reticulocyte lysates (Figures 5B, 3A and B, Table 1) (17,65). Although T116A/T117A/S118A reconstituted telomerase activity *in vitro*, cells containing this mutant did not display elongation activity (Figure 5B, Table 1).

Analysis of mRNA transcript levels confirmed expression of the vector-encoded hygromycin resistance gene at early and late time points in the experiment (Figure 5C). Expression of hTERT(WT), H17A/Y18A/R19A, T116A/T117A/S118A and D868A/D869A alleles was maintained at later population doublings. Expression of Y18A was not maintained (Figure 5C, lanes 7 and 8); thus, we could not formally conclude that this mutant cannot immortalize cells. Notably, Y18A phenocopied H17A/Y18A/R19A *in vitro* and H17A/Y18A/R19A-transduced cells did not survive (Table 1). Q169A was expressed at a lower level than wild-type hTERT in the second experiment, but at a comparable level in the first experiment (Figure 5C, lanes 11 and 12 versus 3 and 4; Supplementary Figure S6, lanes 3 and 4, and 5 and 6 versus lane 2). Regardless of the level of expression, Q169A did not reconstitute activity in lysates (Supplementary Figure S6, lanes 3–5). Therefore, we conclude that hTERT-Q169A cannot immortalize cells (Table 1). Although none of the aforementioned mutants immortalized cells, we did identify mutants that enabled the reconstitution of telomerase activity in lysates and the extension of cellular lifespan (D.C.F. Sealey and M. Taboski unpublished results).

To determine whether mutations in hTEN interfere with the ability of telomerase to maintain telomeres, we analyzed telomere length changes in HA5 stable cell

lines by terminal restriction fragment (TRF) analysis. Average telomere lengths in cells expressing wild-type hTERT were maintained up to population doubling 16 (Figure 5D, lane 4), whereas telomeres in cells expressing H17A/Y18A/R19A, T116A/T117A/S118A, Q169A or D868A/D869A mutants became shorter as the populations reached crises (Figure 5A and D). The average telomere length of cells expressing wild-type hTERT became shorter beyond population doubling 16 (Figure 5D, lanes 5–7), but the population did not encounter crisis (Figure 5A). This result is consistent with the findings of other studies that the maintenance of minimal telomere DNA by hTERT is sufficient for lifespan extension (74,75). Analysis of telomere length changes in cells from the first immortalization experiment (Supplementary Figure S5) revealed similar results (data not shown). Therefore, the mutations in hTEN that we have described render telomerase unable to maintain telomeres and extend cellular lifespan.

DISCUSSION

In this study, we described the ability of the N-terminus of hTERT (hTEN, a.a. 1–200) to interact with telomeric DNA, and complement the activity defect of hTERT(201–1132) + hTR as a separable domain. Mutational analysis identified that Y18 and Q169 residues were required for primer extension activity *in vitro*. These residues, as well as T116/T117/S118, were required for telomere length maintenance and telomerase-mediated extension of cellular lifespan, but not for the interactions of hTEN with DNA or hTERT(201–1132) + hTR.

Many previous studies have used telomerase activity as a read-out for investigating telomerase-primer interactions, in part due to the difficulty of producing sufficient quantities of purified hTERT to measure DNA binding directly. By EMSA (Figures 1C and 2), we demonstrated that the interaction between purified Trx-HIS6-hTERT (1–200) and telomeric DNA was independent of hTR, other domains of hTERT and telomerase activity. The interaction was reproducible across independent purifications of protein and many experimental replicates. The recombinant protein also interacted with hTERT (201–1132) (Supplementary Figure S3). Despite these interactions, Trx-HIS6-hTERT(1–200) produced in bacteria did not regenerate telomerase activity in combination with RRL-hTERT(201–1132) + hTR (Figure 3, Supplementary Figure S3), suggesting that *E. coli* may not provide the folding pathways, modification activities, or binding partners required for telomerase activity that a eukaryotic system can provide (65,76–78). This inability to support catalysis was not due to interference of the N-terminal Trx-HIS6 tag, since Trx-HIS6-hTERT (1–200) produced in RRL conferred a comparable level of telomerase activity as did RRL-produced hTERT(1–200)-S-HIS8 (Supplementary Figure S3). Attempts to activate bacterial Trx-HIS6-hTERT(1–200) with RRL components were unsuccessful (data not shown).

Our method of purification of hTEN represents the most successful of several strategies we attempted. Codon optimization for expression in *E. coli* improved yield significantly (data not shown), but we were unable to obtain enough concentrated Trx-HIS6-hTERT(1–200) to conduct crystallization trials or determine an affinity constant for DNA. In EMSA experiments, we were limited by the total amount and concentration of purified protein, and thus did not observe a quantitative shift of the probe that would be necessary to estimate binding affinities. Nevertheless, we determined the relative affinity of hTEN for DNA oligonucleotides of different sequence and length (Figure 2). DNA 13-nt-long ending in either GGG or GG and containing G residues at specific positions was a preferred substrate for Trx-HIS6-hTERT(1–200) binding, which establishes that hTEN exhibits length and sequence preference for binding telomeric DNA (Figure 2). The sequence specificity of the interaction, changes in the mobility shift upon incubation with anti-HIS antibody, and the lack of DNA-binding activity in *E. coli* lysates expressing Trx-HIS6 alone argue for a specific interaction between purified hTEN and telomeric DNA. The preference of hTEN for telomeric DNA parallels that of endogenous telomerase—a substrate preference that has been, in some instances, attributed to the putative anchor site. For example, oligonucleotides longer than 10–12 nt are necessary for high affinity binding and processive elongation, and substitution of 5' residues (particularly guanines) for non-telomeric residues impairs primer utilization and crosslinking (44–49,79).

Despite the limited sequence similarity among the N-termini of ciliate, yeast and human TERTs (40), the DNA-binding function of the domain appears to be conserved. The recombinant N-termini of Est2 and *Tt*TERT have been shown to interact with DNA in filter binding and crosslinking assays, respectively (40,51,53). Telomerase purified from yeast cells forms crosslinks to DNA via the N-terminus of Est2 (measured in an RNA-dependent assay) (54). Consistently, crosslinking of *Tt*TERT (purified from RRL) to DNA is reduced upon removal of the N-terminus (51,53). Also, the extent of crosslinking of *Tt*TERT to DNA is reduced upon mutation of residues in the N-terminus of *Tt*TERT, including Q168, F178 and W187 (51), and W187 has been identified as a *bona fide* protein contact with telomeric DNA (52). With respect to human telomerase, hTERT(1–300) and (1–350) expressed in reticulocyte lysates can be captured onto biotinylated telomeric DNA [(55), D.C.F. Sealey and L.A. Harrington unpublished results]. The capture of hTERT in this assay is reduced upon removal or mutation of the N-terminus (55). Previous EMSA studies demonstrated an ability of purified ciliate telomerase to bind specifically to telomeric DNA; in this context, telomere DNA binding was TR-dependent (79). To our knowledge, our study represents the first EMSA developed for a specific fragment of recombinant telomerase.

Mutations in the N-termini of TERTs have been identified that impair the activity of human (55,58–63), *T. thermophila* (51,52,80–82) and *S. cerevisiae* telomerases

(40,54,56,57). We identified two mutations in hTERT that attenuated catalytic activity. We targeted hTERT-Q169 for mutation based on the conservation of this residue with *Tt*TERT-Q168 and the position of the latter on the floor of a putative DNA-binding groove on the surface of the N-terminal domain (51). Like *Tt*TERT-Q168A, hTERT-Q169A impaired telomerase activity [(51), Figure 3]; however, unlike *Tt*TERT-Q168A, hTERT-Q169A did not impair DNA binding [(51,52), Figure 4]. This apparent discrepancy may be due to the different assays employed for studying the DNA interaction. Jacobs *et al.* (51) observed that mutation of Q168 reduced the crosslinking of immuno-purified RRL-*Tt*TERT to a 20-nt-long iodouracil-substituted telomeric primer following exposure to UV light and denaturing PAGE. Romi *et al.* (52) observed that mutation of Q168 reduced primer affinity in an assay that measured catalytic activity of RRL-*Tt*TERT following UV-crosslinking to a 6-nt-long iodouracil-substituted telomeric primer. The formation of TERT:DNA crosslinks in these experiments depends on the proximity of iodouracil to reactive amino acid side chains. The interaction between hTEN and an 18-nt-long telomeric primer detected by native gel EMSA was not subject to these parameters. Therefore, whereas previous studies have documented the involvement of *Tt*TERT-Q168 in binding DNA, we did not find similar evidence for hTERT-Q169. Either there are species-specific differences in the function of this conserved residue, or a role for Q169 in binding DNA could not be ascertained by analyzing the behavior of the single amino acid mutant in the native EMSA. Thus, the phenotype of the hTERT-Q169A mutation may be similar to that of *Tt*TERT-D94A and L174A mutations that decrease catalytic activity but not DNA binding/crosslinking (51).

We also identified hTERT-Y18 as a residue (at a non-conserved position but that may lie near the end of the DNA-binding groove) that is required for normal catalytic activity but not necessarily DNA binding (Figures 3 and 4, Supplementary Figure S4). Following from the discussion above, it is possible that Y18 and Q169 do not contact DNA. It is also possible that both Y18 and Q169 contact DNA and can compensate, along with other DNA-binding residues, for the loss of any one DNA contact in a DNA-binding assay. The loss of any one DNA contact may yet render the enzyme incapable of action on a primer. The contributions of Y18 and Q169 to the catalytic reaction cycle may be distinct, given that mutation of each residue impaired activity to a different degree, but the exact contributions of these residues remain to be determined.

Mutation of hTEN at critical sites interfered with the ability of telomerase to immortalize human embryonic kidney cells (Figure 5, Supplementary Figure S5). Residues H17/Y18/R19 and Q169 were required for the generation of telomerase activity in cell lysates, as they were *in vitro*, and also for telomere length maintenance and the continued division of cells in culture. We were not able to formally identify a requirement for Y18 in extending the replicative lifespan of cells because transgene expression was lost during propagation of the

culture (Figure 5C, lanes 7 and 8). Interestingly, the T116A/T117A/S118A triple mutant, which did not exhibit deficits in DNA binding or activity *in vitro* (Figure 4, Table 1), did not regenerate telomerase activity in cell lysates and did not immortalize cells (Figure 5, Supplementary Figure S5). Moriarty *et al.* showed that an hTERT mutant lacking residues 110–119 displays normal activity *in vitro* on telomeric primers 18 nt in length (although repeat addition processivity was reduced on shorter primers), but reduced activity in cell lysates and an inability to immortalize HA5 cells (62,63). Collectively, these results suggest that residues 116–118 may interact with cellular factors that influence recruitment to the telomere or telomerase activity *in vivo*. This possibility is consistent with our prediction that residues 116–118 may be exposed to the non-DNA-binding surface of hTEN (Supplementary Figure S4). By the criteria of Armbruster *et al.* hTERT(T116A/T117A/S118A) fulfills the characteristics of a so-called ‘DAT’ mutation that dissociates the *in vitro* and *in vivo* activities of telomerase (60). The human POT1/TPP1 complex, which interacts with, and can stimulate telomerase, is a candidate modulator of telomerase *in vivo* (38,83), but whether the complex interacts with the N-terminus of hTERT is not known. Notably, *A. thaliana* POT1A interacts with telomerase activity in cells and the N-terminus of *At*TERT *in vitro* (84,85). Several hTERT mutants that displayed no telomerase activity defect *in vitro* were not tested for the ability to immortalize cells (Table 1). It will be interesting to determine if additional mutations in this set have a ‘DAT’ phenotype, which might further define the residues that are required for the *in vivo* functions of telomerase (60).

In addition to binding DNA, hTR and presumably other cellular factors, the N-terminus of hTERT interacts with the C-terminal portion of hTERT in complex with hTR [(59), Figure 3]. Although N- and C-terminal portions of hTERT each contact hTR, hTR or other nucleic acids are not required to bridge this interaction (60,62,86) (Supplementary Figure 3). Co-expression of the N-terminus of hTERT with the hTERT C-terminus–hTR complex reconstitutes active telomerase [(59), Figure 3]. There is also evidence to suggest that C-terminal regions of TERT interact with DNA [(51–53,55,87) D.C.F. Sealey and L.A. Harrington unpublished results], and that C-terminal regions are required for normal telomerase function *in vitro* and *in vivo* (58,61,87–89). Thus, it is possible that N- and C-terminal regions of TERT combine to form one DNA-binding site. Alternatively, N- and C-terminal regions of TERT may bind DNA separately, but in a cooperative manner. In the latter scenario, the N-terminus of TERT, which has been described as a low affinity DNA-binding domain (53), may not recruit telomerase to primers, but once DNA is bound to another site in hTERT, the local concentration of DNA available to the N-terminus may be sufficiently high for a stable interaction to occur. In turn, the N-terminus may contribute specificity (Figure 2), along with the RNA template in hTR, to the primer sequences that can be bound and elongated efficiently by telomerase. This hypothesis is consistent with the crosslinking of

E. aediculatus telomerase to primers at both 5'- and 3'-ends (49), and the observation that telomerase cannot extend short primers or primers with non-G-rich 5'-ends efficiently (44–48,90). Finally, whether the functional multimerization of N- and C-terminal regions of hTERT reflects an intra- or inter-molecular interaction in the context of native telomerase remains to be determined.

The exact telomerase reaction mechanism has yet to be fully elucidated. Structure–function analysis is beginning to shed light on how various domains of TERT, TR, other proteins and telomeric DNA associate and work together. For example, *Tt*TERT-W187 can crosslink to the same nucleotide in telomeric primers with different registers, suggesting that N-terminus of TERT may form a static interaction with DNA during each round of RNA template copying (52). The sequence-specificity of the DNA interaction with the N-terminus of hTERT at different nucleotide positions may reflect this property (Figure 2). Also, mutation of *Tt*TERT-L14 impairs telomere repeat addition processivity but not DNA binding, which led Zaug *et al.* (82) to propose models of how the N-terminus may behave during primer translocation. These findings, along with the knowledge that *Tt*TERT-Q168, the N-terminus of Est2, and now human TERT-Q169 and Y18 are required for productive elongation of DNA [(51,52,57), Figure 3], are beginning to inform an understanding of the molecular events of the telomerase reaction cycle. Deciphering exactly how the N-terminus of hTERT enables telomerase function may provide an additional target for inhibiting telomerase function in cancer.

NOTE ADDED IN REVISION

While this article was under review, Wyatt *et al.* (91) reported that mutation of hTERT-Q169 impairs telomerase catalytic activity *in vitro*. The Q169A mutation did not reduce the interaction of RRL-expressed hTERT(1–300) with (TTAGGG)₃ in a biotinylated DNA pull-down assay, but did reduce the interaction with (TTAGGG)₂ and TTAGGG primers. Further, hTERT(Q169A) did not restore telomerase activity, or confer lifespan extension or telomere maintenance to telomerase-negative cells. Thus, these findings are consistent with the present study.

SUPPLEMENTARY DATA

Supplementary Data are available at NAR Online.

ACKNOWLEDGEMENTS

The authors thank Dr Tom Cech, Dr Elaine Podell, Dr Art Zaug, Dr Chris Marshall, Carol Liu, Dr Linda Holland, Dr Susan McCracken, Dr Fiona Pryde, Dr Laura Gardano, Dr Steve Innocente, Jen Dorrens and Dr Rob Laister for technical assistance, advice, or sharing unpublished data. They thank Theo Goh and Dr Thierry LeBihan for mass spectrometry analysis of purified, recombinant hTERT.

FUNDING

National Cancer Institute of Canada (NCIC15072 to L.H.); the National Institutes of Health (AG02398-05 to L.H.); the Wellcome Trust (WT84637 to L.H.); the Canadian Institutes of Health Research (MT-13611 to M.I.); and the Canada Foundation for Innovation. We thank T.W. Mak for transitional funding from the Campbell Family Institute for Breast Cancer Research. Funding for open access charge: Wellcome Trust.

Conflict of interest statement. None declared.

REFERENCES

- De Lange, T., Lundblad, V. and Blackburn, E.H. (2006) *Telomeres*, 2nd edn. Cold Spring Harbor Laboratory Press, Cold Spring Harbor, NY.
- Griffith, J.D., Comeau, L., Rosenfield, S., Stansel, R.M., Bianchi, A., Moss, H. and de Lange, T. (1999) Mammalian telomeres end in a large duplex loop. *Cell*, **97**, 503–514.
- Nikitina, T. and Woodcock, C.L. (2004) Closed chromatin loops at the ends of chromosomes. *J. Cell Biol.*, **166**, 161–165.
- Palm, W. and de Lange, T. (2008) How shelterin protects mammalian telomeres. *Annu. Rev. Genet.*, **42**, 301–334.
- Denchi, E.L. and de Lange, T. (2007) Protection of telomeres through independent control of ATM and ATR by TRF2 and POT1. *Nature*, **448**, 1068–1071.
- Watson, J.D. (1972) Origin of concatemeric T7 DNA. *Nat. New Biol.*, **239**, 197–201.
- Olovnikov, A.M. (1973) A theory of marginotomy. The incomplete copying of template margin in enzymic synthesis of polynucleotides and biological significance of the phenomenon. *J. Theor. Biol.*, **41**, 181–190.
- Jacob, N.K., Kirk, K.E. and Price, C.M. (2003) Generation of telomeric G strand overhangs involves both G and C strand cleavage. *Mol. Cell*, **11**, 1021–1032.
- Sfeir, A.J., Chai, W., Shay, J.W. and Wright, W.E. (2005) Telomere-end processing the terminal nucleotides of human chromosomes. *Mol. Cell*, **18**, 131–138.
- Harley, C.B., Futcher, A.B. and Greider, C.W. (1990) Telomeres shorten during ageing of human fibroblasts. *Nature*, **345**, 458–460.
- d'Adda di Fagagna, F., Reaper, P.M., Clay-Farrace, L., Fiegler, H., Carr, P., Von Zglinicki, T., Saretzki, G., Carter, N.P. and Jackson, S.P. (2003) A DNA damage checkpoint response in telomere-initiated senescence. *Nature*, **426**, 194–198.
- Herbig, U., Jobling, W.A., Chen, B.P., Chen, D.J. and Sedivy, J.M. (2004) Telomere shortening triggers senescence of human cells through a pathway involving ATM, p53, and p21(CIP1), but not p16(INK4a). *Mol. Cell*, **14**, 501–513.
- Greider, C.W. and Blackburn, E.H. (1985) Identification of a specific telomere terminal transferase activity in Tetrahymena extracts. *Cell*, **43**, 405–413.
- Feng, J., Funk, W.D., Wang, S.S., Weinrich, S.L., Avilion, A.A., Chiu, C.P., Adams, R.R., Chang, E., Allsopp, R.C., Yu, J. *et al.* (1995) The RNA component of human telomerase. *Science*, **269**, 1236–1241.
- Nakamura, T.M., Morin, G.B., Chapman, K.B., Weinrich, S.L., Andrews, W.H., Lingner, J., Harley, C.B. and Cech, T.R. (1997) Telomerase catalytic subunit homologs from fission yeast and human. *Science*, **277**, 955–959.
- Meyerson, M., Counter, C.M., Eaton, E.N., Ellisen, L.W., Steiner, P., Caddle, S.D., Ziaugra, L., Beijersbergen, R.L., Davidoff, M.J., Liu, Q. *et al.* (1997) hEST2, the putative human telomerase catalytic subunit gene, is up-regulated in tumor cells and during immortalization. *Cell*, **90**, 785–795.
- Harrington, L., Zhou, W., McPhail, T., Oulton, R., Yeung, D.S., Mar, V., Bass, M.B. and Robinson, M.O. (1997) Human telomerase contains evolutionarily conserved catalytic and structural subunits. *Genes Dev.*, **11**, 3109–3115.
- Kilian, A., Bowtell, D.D., Abud, H.E., Hime, G.R., Venter, D.J., Keese, P.K., Duncan, E.L., Reddel, R.R. and Jefferson, R.A. (1997) Isolation of a candidate human telomerase catalytic subunit gene, which reveals complex splicing patterns in different cell types. *Hum. Mol. Genet.*, **6**, 2011–2019.
- Nakayama, J., Tahara, H., Tahara, E., Saito, M., Ito, K., Nakamura, H., Nakanishi, T., Ide, T. and Ishikawa, F. (1998) Telomerase activation by hTERT in human normal fibroblasts and hepatocellular carcinomas. *Nat. Genet.*, **18**, 65–68.
- Armanios, M. (2009) Syndromes of telomere shortening. *Annu. Rev. Genomics Hum. Genet.* doi:10.1016/j.ajhg.2009.10.028.
- Kim, N.W., Piatyszek, M.A., Prowse, K.R., Harley, C.B., West, M.D., Ho, P.L., Coviello, G.M., Wright, W.E., Weinrich, S.L. and Shay, J.W. (1994) Specific association of human telomerase activity with immortal cells and cancer. *Science*, **266**, 2011–2015.
- Campisi, J. (2005) Senescent cells, tumor suppression, and organismal aging: good citizens, bad neighbors. *Cell*, **120**, 513–522.
- Artandi, S.E. and DePinho, R.A. (2000) A critical role for telomeres in suppressing and facilitating carcinogenesis. *Curr. Opin. Genet. Dev.*, **10**, 39–46.
- Shay, J.W. and Bacchetti, S. (1997) A survey of telomerase activity in human cancer. *Eur. J. Cancer*, **33**, 787–791.
- Cesare, A.J. and Reddel, R.R. (2008) Telomere uncapping and alternative lengthening of telomeres. *Mech. Ageing Dev.*, **129**, 99–108.
- Bodnar, A.G., Ouellette, M., Frolkis, M., Holt, S.E., Chiu, C.P., Morin, G.B., Harley, C.B., Shay, J.W., Lichtsteiner, S. and Wright, W.E. (1998) Extension of life-span by introduction of telomerase into normal human cells. *Science*, **279**, 349–352.
- Vaziri, H. and Benchimol, S. (1998) Reconstitution of telomerase activity in normal human cells leads to elongation of telomeres and extended replicative life span. *Curr. Biol.*, **8**, 279–282.
- Sealey, D., Zakian, V. and Harrington, L. (2006) In DePamphilis, M. (ed.), *DNA Replication and Human Disease*. Cold Spring Harbor Laboratory Press, Cold Spring Harbor, pp. 561–591.
- Kyron, G., Boakye, K.A. and Lustig, A.J. (1992) C-terminal truncation of RAP1 results in the deregulation of telomere size, stability, and function in *Saccharomyces cerevisiae*. *Mol. Cell Biol.*, **12**, 5159–5173.
- Wotton, D. and Shore, D. (1997) A novel Rap1p-interacting factor, Rif2p, cooperates with Rif1p to regulate telomere length in *Saccharomyces cerevisiae*. *Genes Dev.*, **11**, 748–760.
- van Steensel, B. and de Lange, T. (1997) Control of telomere length by the human telomeric protein TRF1. *Nature*, **385**, 740–743.
- Smogorzewska, A., van Steensel, B., Bianchi, A., Oelmann, S., Schaefer, M.R., Schnapp, G. and de Lange, T. (2000) Control of human telomere length by TRF1 and TRF2. *Mol. Cell Biol.*, **20**, 1659–1668.
- Teixeira, M.T., Arneric, M., Sperisen, P. and Lingner, J. (2004) Telomere length homeostasis is achieved via a switch between telomerase-extendible and -nonextendible states. *Cell*, **117**, 323–335.
- Loayza, D. and De Lange, T. (2003) POT1 as a terminal transducer of TRF1 telomere length control. *Nature*, **423**, 1013–1018.
- Lei, M., Podell, E.R. and Cech, T.R. (2004) Structure of human POT1 bound to telomeric single-stranded DNA provides a model for chromosome end-protection. *Nat. Struct. Mol. Biol.*, **11**, 1223–1229.
- Lei, M., Zaug, A.J., Podell, E.R. and Cech, T.R. (2005) Switching human telomerase on and off with hPOT1 protein in vitro. *J. Biol. Chem.*, **280**, 20449–20456.
- Kelleher, C., Kurth, I. and Lingner, J. (2005) Human protection of telomeres 1 (POT1) is a negative regulator of telomerase activity in vitro. *Mol. Cell Biol.*, **25**, 808–818.
- Wang, F., Podell, E.R., Zaug, A.J., Yang, Y., Baciou, P., Cech, T.R. and Lei, M. (2007) The POT1-TPP1 telomere complex is a telomerase processivity factor. *Nature*, **445**, 506–510.
- Kelleher, C., Teixeira, M.T., Forstmann, K. and Lingner, J. (2002) Telomerase: biochemical considerations for enzyme and substrate. *Trends Biochem. Sci.*, **27**, 572–579.

40. Xia, J., Peng, Y., Mian, I.S. and Lue, N.F. (2000) Identification of functionally important domains in the N-terminal region of telomerase reverse transcriptase. *Mol. Cell Biol.*, **20**, 5196–5207.
41. Bosoy, D. and Lue, N.F. (2004) Yeast telomerase is capable of limited repeat addition processivity. *Nucleic Acids Res.*, **32**, 93–101.
42. Greider, C.W. (1991) Telomerase is processive. *Mol. Cell Biol.*, **11**, 4572–4580.
43. Prowse, K.R., Avilion, A.A. and Greider, C.W. (1993) Identification of a nonprocessive telomerase activity from mouse cells. *Proc. Natl Acad. Sci. USA*, **90**, 1493–1497.
44. Morin, G.B. (1989) The human telomere terminal transferase enzyme is a ribonucleoprotein that synthesizes TTAGGG repeats. *Cell*, **59**, 521–529.
45. Morin, G.B. (1991) Recognition of a chromosome truncation site associated with alpha-thalassaemia by human telomerase. *Nature*, **353**, 454–456.
46. Harrington, L.A. and Greider, C.W. (1991) Telomerase primer specificity and chromosome healing. *Nature*, **353**, 451–454.
47. Collins, K. and Greider, C.W. (1993) Tetrahymena telomerase catalyzes nucleolytic cleavage and nonprocessive elongation. *Genes Dev.*, **7**, 1364–1376.
48. Lee, M.S. and Blackburn, E.H. (1993) Sequence-specific DNA primer effects on telomerase polymerization activity. *Mol. Cell Biol.*, **13**, 6586–6599.
49. Hammond, P.W., Lively, T.N. and Cech, T.R. (1997) The anchor site of telomerase from *Euplotes aediculatus* revealed by photo-cross-linking to single- and double-stranded DNA primers. *Mol. Cell Biol.*, **17**, 296–308.
50. Lue, N.F. (2004) Adding to the ends: what makes telomerase processive and how important is it? *Bioessays*, **26**, 955–962.
51. Jacobs, S.A., Podell, E.R. and Cech, T.R. (2006) Crystal structure of the essential N-terminal domain of telomerase reverse transcriptase. *Nat. Struct. Mol. Biol.*, **13**, 218–225.
52. Romi, E., Baran, N., Gantman, M., Shmoish, M., Min, B., Collins, K. and Manor, H. (2007) High-resolution physical and functional mapping of the template adjacent DNA binding site in catalytically active telomerase. *Proc. Natl Acad. Sci. USA*, **104**, 8791–8796.
53. Finger, S.N. and Bryan, T.M. (2008) Multiple DNA-binding sites in Tetrahymena telomerase. *Nucleic Acids Res.*, **36**, 1260–1272.
54. Lue, N.F. (2005) A physical and functional constituent of telomerase anchor site. *J. Biol. Chem.*, **280**, 26586–26591.
55. Wyatt, H.D., Lobb, D.A. and Beattie, T.L. (2007) Characterization of physical and functional anchor site interactions in human telomerase. *Mol. Cell Biol.*, **27**, 3226–3240.
56. Friedman, K.L. and Cech, T.R. (1999) Essential functions of amino-terminal domains in the yeast telomerase catalytic subunit revealed by selection for viable mutants. *Genes Dev.*, **13**, 2863–2874.
57. Lue, N.F. and Li, Z. (2007) Modeling and structure function analysis of the putative anchor site of yeast telomerase. *Nucleic Acids Res.*, **35**, 5213–5222.
58. Beattie, T.L., Zhou, W., Robinson, M.O. and Harrington, L. (2000) Polymerization defects within human telomerase are distinct from telomerase RNA and TEP1 binding. *Mol. Biol. Cell*, **11**, 3329–3340.
59. Beattie, T.L., Zhou, W., Robinson, M.O. and Harrington, L. (2001) Functional multimerization of the human telomerase reverse transcriptase. *Mol. Cell Biol.*, **21**, 6151–6160.
60. Armbruster, B.N., Banik, S.S., Guo, C., Smith, A.C. and Counter, C.M. (2001) N-terminal domains of the human telomerase catalytic subunit required for enzyme activity in vivo. *Mol. Cell Biol.*, **21**, 7775–7786.
61. Lee, S.R., Wong, J.M. and Collins, K. (2003) Human telomerase reverse transcriptase motifs required for elongation of a telomeric substrate. *J. Biol. Chem.*, **278**, 52531–52536.
62. Moriarty, T.J., Marie-Egyptienne, D.T. and Autexier, C. (2004) Functional organization of repeat addition processivity and DNA synthesis determinants in the human telomerase multimer. *Mol. Cell Biol.*, **24**, 3720–3733.
63. Moriarty, T.J., Ward, R.J., Taboski, M.A. and Autexier, C. (2005) An anchor site-type defect in human telomerase that disrupts telomere length maintenance and cellular immortalization. *Mol. Biol. Cell*, **16**, 3152–3161.
64. Weinrich, S.L., Pruzan, R., Ma, L., Ouellette, M., Tesmer, V.M., Holt, S.E., Bodnar, A.G., Lichtsteiner, S., Kim, N.W., Trager, J.B. et al. (1997) Reconstitution of human telomerase with the template RNA component hTR and the catalytic protein subunit hTRT. *Nat. Genet.*, **17**, 498–502.
65. Beattie, T.L., Zhou, W., Robinson, M.O. and Harrington, L. (1998) Reconstitution of human telomerase activity in vitro. *Curr. Biol.*, **8**, 177–180.
66. Turchin, A. and Lawler, J.F. Jr (1999) The primer generator: a program that facilitates the selection of oligonucleotides for site-directed mutagenesis. *Biotechniques*, **26**, 672–676.
67. Hayflick, L. (1973) In Kruze, P.F. and Patterson, M.K. (eds), *Tissue Culture: Methods and Applications*. Academic Press, New York, pp. 220–223.
68. Chai, W., Shay, J.W. and Wright, W.E. (2005) Human telomeres maintain their overhang length at senescence. *Mol. Cell Biol.*, **25**, 2158–2168.
69. Sinquett, F.L., Dryer, R.L., Marcelli, V., Batheja, A. and Covey, L.R. (2009) Single nucleotide changes in the human Iggamma1 and Iggamma4 promoters underlie different transcriptional responses to CD40. *J. Immunol.*, **182**, 2185–2193.
70. Dempsey, L.A., Hanakahi, L.A. and Maizels, N. (1998) A specific isoform of hnRNP D interacts with DNA in the LR1 heterodimer: canonical RNA binding motifs in a sequence-specific duplex DNA binding protein. *J. Biol. Chem.*, **273**, 29224–29229.
71. Hanakahi, L.A., Dempsey, L.A., Li, M.J. and Maizels, N. (1997) Nucleolin is one component of the B cell-specific transcription factor and switch region binding protein, LR1. *Proc. Natl Acad. Sci. USA*, **94**, 3605–3610.
72. Counter, C.M., Avilion, A.A., LeFeuvre, C.E., Stewart, N.G., Greider, C.W., Harley, C.B. and Bacchetti, S. (1992) Telomere shortening associated with chromosome instability is arrested in immortal cells which express telomerase activity. *EMBO J.*, **11**, 1921–1929.
73. Kim, M., Xu, L. and Blackburn, E.H. (2003) Catalytically active human telomerase mutants with allele-specific biological properties. *Exp. Cell Res.*, **288**, 277–287.
74. Zhu, J., Wang, H., Bishop, J.M. and Blackburn, E.H. (1999) Telomerase extends the lifespan of virus-transformed human cells without net telomere lengthening. *Proc. Natl Acad. Sci. USA*, **96**, 3723–3728.
75. Ouellette, M.M., Liao, M., Herbert, B.S., Johnson, M., Holt, S.E., Liss, H.S., Shay, J.W. and Wright, W.E. (2000) Subsenescent telomere lengths in fibroblasts immortalized by limiting amounts of telomerase. *J. Biol. Chem.*, **275**, 10072–10076.
76. Bachand, F. and Autexier, C. (1999) Functional reconstitution of human telomerase expressed in *Saccharomyces cerevisiae*. *J. Biol. Chem.*, **274**, 38027–38031.
77. Holt, S.E., Aisner, D.L., Baur, J., Tesmer, V.M., Dy, M., Ouellette, M., Trager, J.B., Morin, G.B., Toft, D.O., Shay, J.W. et al. (1999) Functional requirement of p23 and Hsp90 in telomerase complexes. *Genes Dev.*, **13**, 817–826.
78. Masutomi, K., Kaneko, S., Hayashi, N., Yamashita, T., Shirota, Y., Kobayashi, K. and Murakami, S. (2000) Telomerase activity reconstituted in vitro with purified human telomerase reverse transcriptase and human telomerase RNA component. *J. Biol. Chem.*, **275**, 22568–22573.
79. Harrington, L., Hull, C., Crittenden, J. and Greider, C. (1995) Gel shift and UV cross-linking analysis of Tetrahymena telomerase. *J. Biol. Chem.*, **270**, 8893–8901.
80. Miller, M.C., Liu, J.K. and Collins, K. (2000) Template definition by Tetrahymena telomerase reverse transcriptase. *EMBO J.*, **19**, 4412–4422.
81. Jacobs, S.A., Podell, E.R., Wuttke, D.S. and Cech, T.R. (2005) Soluble domains of telomerase reverse transcriptase identified by high-throughput screening. *Protein Sci.*, **14**, 2051–2058.

82. Zaug,A.J., Podell,E.R. and Cech,T.R. (2008) Mutation in TERT separates processivity from anchor-site function. *Nat. Struct. Mol. Biol.*, **15**, 870–872.
83. Xin,H., Liu,D., Wan,M., Safari,A., Kim,H., Sun,W., O'Connor,M.S. and Songyang,Z. (2007) TPP1 is a homologue of ciliate TEBP-beta and interacts with POT1 to recruit telomerase. *Nature*, **445**, 559–562.
84. Rossignol,P., Collier,S., Bush,M., Shaw,P. and Doonan,J.H. (2007) Arabidopsis POT1A interacts with TERT-V(18), an N-terminal splicing variant of telomerase. *J. Cell Sci.*, **120**, 3678–3687.
85. Surovtseva,Y.V., Shakirov,E.V., Vespa,L., Osbun,N., Song,X. and Shippen,D.E. (2007) Arabidopsis POT1 associates with the telomerase RNP and is required for telomere maintenance. *EMBO J.*, **26**, 3653–3661.
86. Arai,K., Masutomi,K., Khurts,S., Kaneko,S., Kobayashi,K. and Murakami,S. (2002) Two independent regions of human telomerase reverse transcriptase are important for its oligomerization and telomerase activity. *J. Biol. Chem.*, **277**, 8538–8544.
87. Hossain,S., Singh,S. and Lue,N.F. (2002) Functional analysis of the C-terminal extension of telomerase reverse transcriptase. A putative “thumb” domain. *J. Biol. Chem.*, **277**, 36174–36180.
88. Banik,S.S., Guo,C., Smith,A.C., Margolis,S.S., Richardson,D.A., Tirado,C.A. and Counter,C.M. (2002) C-terminal regions of the human telomerase catalytic subunit essential for in vivo enzyme activity. *Mol. Cell. Biol.*, **22**, 6234–6246.
89. Huard,S., Moriarty,T.J. and Autexier,C. (2003) The C terminus of the human telomerase reverse transcriptase is a determinant of enzyme processivity. *Nucleic Acids Res.*, **31**, 4059–4070.
90. Greider,C.W. and Blackburn,E.H. (1987) The telomere terminal transferase of Tetrahymena is a ribonucleoprotein enzyme with two kinds of primer specificity. *Cell*, **51**, 887–898.
91. Wyatt. *et al.* (2009) Human telomerase reverse transcriptase (hTERT) Q169 is essential for telomerase function in vitro and in vivo. *PLoS ONE*, **4**, e7176.